Ritthichai Ratchapan[1], Somchai Kriprab[1], Supapradit Marsong[1], Boonyang Plangklang[1,*], Yuttana Kongjeen[2]

Rajamangala University of Technology Thanyaburi, Thailand (1),
Rajamangala University of Technology Isan, Nakhon Ratchasima, Thailand (2)

doi:10.15199/48.2024.01.03

An Analysis of the Ampacity and Capital Costs for Underground High Voltage Power Cable Construction Methods

Abstract. *This study aimed to evaluate the ampacity and costs of different high voltage underground cable methods (cylindrical duct bank vs. square tunnel). The standards of Metropolitan Electricity Authority (MEA) of Thailand innovative approach to reduce road impact were used. Simulations for 115 kV cables showed that the maximum ampacity for cylindrical duct bank method was 523 A (flooding), and 509 A (non-flooding) while that of the square tunnel method was 445 A (flooding), and 405 A (non-flooding). Costs analysis were $573,446 per circuit for the cylindrical duct bank method and $404,363 per circuit for the square tunnel method.*

Streszczenie. *Celem tego badania była ocena obciążalności prądowej i kosztów różnych metod podziemnych kabli wysokiego napięcia (cylindryczny zespół kanałów vs. tunel kwadratowy). Wykorzystano standardy Metropolitan Electricity Authority (MEA) Tajlandii, innowacyjne podejście do zmniejszania wpływu na drogę. Symulacje dla kabli 115 kV wykazały, że maksymalna obciążalność prądowa dla metody cylindrycznej wiązki przewodów wynosiła 523 A (zalanie) i 509 A (bez zalania), natomiast dla metody tunelu kwadratowego wyniosła 445 A (zalanie) i 405 A (niezalanie). powódź). Analiza kosztów wyniosła 573 446 USD na obwód w przypadku metody z kanałem cylindrycznym i 404 363 USD na obwód w przypadku metody z tunelem kwadratowym.* (***Analiza obciążalności prądowej i kosztów inwestycyjnych metod budowy podziemnych kabli elektroenergetycznych wysokiego napięcia***)

Keywords: Ampacity, Cylindrical duct bank, Capital cost, Square tunnel, Underground power cable
Słowa kluczowe: Natężenie prądu, Cylindryczny zestaw kanałów, Koszt inwestycyjny, Tunel kwadratowy, Podziemny kabel zasilający

Introduction

In contemporary times, the transmission line systems in electrical power networks play a pivotal role in catering to the needs of end-users. In sprawling urban centers, the task of procuring electricity from external sources and subsequently transmitting it to central areas for equitable load distribution remains paramount. With the swift expansion of urban areas and escalating energy consumption rates, the conventional transmission line systems face challenges. To address these challenges, the deployment of underground cables has emerged as a viable alternative to conventional methods, such as direct burial, semi-direct burial, open cut, horizontal direction drilling (HDD), pipe jacking, and tunneling [1, 2].In order for the operational system to function effectively, advancements in the transportation sector, material technology, and electronic devices play a crucial role as they require electric power to operate. The optimal condition of the grid necessitates energy management, which involves both preparation and control.

To effectively manage the power services, it is essential to highlight the key features of the electrical system. In Thailand, the power service providers are structured into three distinct organizations. These entities consist of the Electricity Generating Authority of Thailand (EGAT), the Metropolitan Electricity Authority (MEA) of Thailand, and the Provincial Electricity Authority of Thailand (PEA). Specifically, MEA caters to the electrical system service provision in central regions such as Bangkok, Nonthaburi, and Samut-Prakan province [3]. Previously, researchers have demonstrated using XLPE cable in direct burial applications [4] .The direct burial offers the advantage of rapid installation, and the XLPE cable can effectively transfer heat to the soil, which is associated with high ampacity.

However, the XLPE cable can be easily damaged by physical factors. To install underground cables using the open-cut method, a reinforced concrete covering is applied over High-Density Polyethylene (HDPE) and metal conduit. This approach is commonly chosen for installation in rural and spacious urban areas. The open-cut method serves as a safeguard against mechanical damage [5]. On the other hand, (Horizontal Directional Drilling) HDD method has been employed for the construction of underground power cables to navigate obstacles or cross rivers [6, 7]. However, this approach necessitates precise positioning at the opposite manhole.

The tunneling method has been adopted for the construction of tunnels to accommodate large-scale power cables. This approach is well-suited for numerous electrical circuits and long-distance transmission line systems. One of the advantages of the tunneling method is the provision of ventilated air within the tunnels [8, 9].Meanwhile, the capital cost is higher and construction period is long. Pipe jacking method is used for utility support such as cold water, telecommunication, wastewater drainage system, electrical power system, etc. [10].The primary construction approach utilized is pipe jacking, a widely favoured technique renowned for its substantial reduction in traffic and public disturbances. Pipe jacking method effectively prevents mechanical stress and enhances strength *of* infrastructure. Key determinants, including cable ampacity and construction methods, significantly impact project costs. Hence, conducting an ampacity study for the installation method is crucial to ensuring reliable power system design. Furthermore, both internal and external heat sources have directly influence on the ampacity of the XLPE cable. The internal heat sources include conductor temperature, cable void space, cable jacket, conduit void space, conduit material, reinforced concrete duct bank, soil properties, and ambient temperature, as outlined in reference [11]. Determinants of XLPE cable ampacity heavily rely on heat dissipation. The dimensions of duct banks directly influence XLPE cable heat dissipation [12]. Modifying cable spacing can decrease heat accumulation in XLPE cables. Furthermore, altering cable arrangement can reduce conductor heat storage. Consequently, flat formation arrangement results in higher ampacity than trefoil formation [13]. The impact of ambient temperature on conductor cooling is significant. If the ambient temperature is high, the ampacity of the XLPE cable will be reduced [14]. Heat flow during fires has been presented by using the wire heat flow during excessive thermal conditions with fire conditions to understand copper conductor heat flow. Model

developed to estimate wire temperature based on heating time and distance from heat source [15]. Heat exchange in cables was discussed by the heat exchange in cables exceeding permissible temperatures. The temperature model of electrical cable was used by distributed parameters based on exposure duration and distance from heat source [16].The paper discusses the temperature restriction called the 2 K-criterion for the installation of submarine cables in the German North Sea or Baltic Sea, which limits the heating of the seabed by the cable losses to 2.0 K. This criterion has significant effects on cable design, requiring greater laying depths and potentially more expensive cables with larger conductor cross-sections [17].The formation of dry zones around underground cables decreases their capacity by a factor of 0.87 to 0.96, depending on the type of soil. This factor is defined as the derating factor. The drying zone in backfill starts at different temperatures and velocities depending on the type of soil and the weight percentage of silt. The time required for the formation of the dry zone is longer for sand samples containing silt compared to those without silt. The velocity of the movement of the dry zone is also slower in sand with silt [18].The paper presents an optimal RC ladder-type equivalent circuit for the representation of the soil for dynamic thermal rating of underground cable installations, which is compatible with the International Electrotechnical Commission thermal-electric analog circuits for cables. The model has been optimized through a comprehensive parametric analysis and it has been determined that a model of order five can represent all typical transients on common installations. The model represents a relevant improvement to the available operation and monitoring tools for underground cables, making them more efficient and robust [19].The effect of changing cable arrangements near a substation and the two-point bonding of sheaths on the calculations of circulating current sheath loss factors and resulting circuit ratings. The calculations of complex impedance matrix formulations (CIM) were used calculation of sheath loss factors in cross-bonded systems that related by the potential hazardous effect of neglecting the change in cable arrangements at the terminations on the calculated circulating current sheath loss factors and circuit ratings [20].Mathematical model for XLPE insulated underground power cable was represented by behaviour considering factors such as dielectric losses, ambient temperature, and cable core resistance [21]. Factors influencing of power cable was most affected current-carrying capacity including soil parameters, external heat, and cable positioning [22]. The underground power cables with intersections methods have been considered safe design to achieve rated currents-carrying capacity with minimizing the effects of combined heat [23].

Meanwhile, soil moisture can increase the cable ampacity. On the contrary, the larger the depth of the underground power cables, the greater distance for cooling and the lower the ampacity of the cable [24].Conversely, precipitation can reduce soil heat resistance, enabling underground cables to support heavier loads over a brief span [25]. Additionally, the dimensions of duct banks play a crucial role in influencing ampacity, construction costs, and cable losses [26].In addition, the heat removal of underground cables using Hydronic Asphalt Pavement (HAP) and Hydronic Concrete Pavement (HCP) has been studied and improved by using backfill material. Backfill material has also been replaced with a higher thermal conductivity material for the cable to conduct maximum current. Although HAP and HCP are needed to increase the ampacity of the underground power cables, they raise the construction cost. Meanwhile, the payback period is short [27, 28]. However, the challenges of cylindrical duct bank using the pipe jacking method limitation on the number of circuits, impact on the electrical system, and traffic area restoration. Consequently, considering the congested traffic conditions as depicted in Figure 1, the square tunnel using the pipe jacking method is chosen to moderate the impact from the cylindrical duct bank.

In the context of Bangkok, Thailand, the construction of underground power cables is of considerable significance. This paper aims to explore an effective method for addressing the inherent challenges in this construction process, with a specific focus on reducing construction costs and optimizing ampacity. To achieve this, a comprehensive was performed on various methods for constructing underground power cables and their respective impacts on construction expenses and ampacity performance assessed.

The subsequent sections of this paper are organized as follows: Section 2 delves into the formulation of the problems at hand. Section 3 details the proposed approach and provides an illustrative case study showcasing its application. Section 4 presents the outcomes of simulations, offering empirical evidence of the method's efficacy. Finally, Section 5 presents our conclusions, drawn from the study's findings, emphasizing the significance of our proposed approach within the context of underground power cable construction.

Fig.1. Road traffic heavily influences the transmission line construction in urban areas

Analysis of Underground Power Cables

This research is performed using the finite element method (FEM) and a 2D steady-state thermal analysis. The FEM equations are expressed as follows [27, 28]:

$$(1) \qquad \frac{\partial}{\partial x}\left(k.\frac{\partial T}{\partial x}\right)+\frac{\partial}{\partial x}\left(k.\frac{\partial T}{\partial x}\right)+Q_v=0$$

The volume power of heat source in the cable conductor can be shown as follows [27, 28].

$$(2) \qquad Q_v=\frac{R_{ac}(T_{cp})}{S_c}I^2$$

Large computational domain uses the zero-heat flux boundary condition, consisting of the left, bottom and right

sides. The zero heat flux can be expressed by the following equation [27, 28].

$$k\frac{\partial T}{\partial n}=0 \quad (3)$$

The ability of a high-voltage underground cable to carry current is influenced by several factors, including the number of cables, the types of cables used, cable construction, materials, the cable placement in the ground, and the arrangement of cable bonding. The equation that determines the cable current-carrying capacity takes into account both steady-state and transient conditions. This paper focused on the steady-state condition for buried cables, without considering moisture migration, which is represented by Equation (4). Additionally, the paper also addressed the condition with moisture migration, and the corresponding equation is represented as equation (13).

$$I=\left[\frac{\Delta\theta-W_d\left[0.5T+n\left(T_2+T_3+T_4\right)_1\right]}{RT_1+nR(1+\lambda_1)T_2+nR(1+\lambda_1+\lambda_2)\left(T_3+T_4\right)}\right]^{0.5} \quad (4)$$

where R is the ac resistance per unit length of the conductor at the maximum operating temperature. W_c, W_d, W_s, and W_a represent the conductor, dielectric, sheath, and armor losses in W/m, respectively. T_1 is the thermal resistance per unit length between one conductor and sheath. T_2 is the thermal resistance per unit length of the bedding between sheath and armor. T_3 is the thermal resistance per unit length of the external serving of the cable. $T_4$is the thermal resistance per length between the cable surface and the surrounding medium. $\lambda_1$is the sheath loss factor. λ_2 is the armor loss factor. n is the number of load-carrying conductor in the power cables.

The heat transfer in the cable is expressed by the internal and external condition as follows.

$$T=\frac{T_1}{n}+\left(1+\lambda_1\right)T_2+\left(1+\lambda_1+\lambda_2\right)T_3 \quad (5)$$

$$T_d=\frac{T_1}{2n}+T_2+T_3 \quad (6)$$

Therefore, equation (4) becomes.

$$\Delta\theta=n\left(W_cT+W_tT_4+W_dT_d\right) \quad (7)$$

where W_t are the total losses generated in the cable defined by:

$$W_t=W_t+W_d=W_c\left(1+\lambda_1+\lambda_2\right)+W_d \quad (8)$$

The T can be computed by equation (5), which is provided by an equivalent cable thermal resistance. Therefore, the internal resistance of the cable is depended on the cable construction method. Meanwhile, the external thermal resistance depends on the properties of the surrounding medium on the overall cable diameter. Therefore, the thermal resistance of the power cable is related to the thermal resistance per unit length between the cable surface and the surrounding medium T_4 as follows.

$$T_4=T_4^{'}+T_4^{''}+T_4^{'''} \quad (9)$$

where T_4 is the thermal resistance of the air or liquid between the cable surface and the duct internal surface. T_4 $T_4^{''}$is the thermal resistance of the duct itself. $T_4$is the external thermal resistance of the duct. Those are expressed as follows.

$$T_4^{'}=\frac{U}{1+01\left(V+Y\theta_m\right)D_e} \quad (10)$$

where U , V and Y constants are defined by referring to IEC 60287 standard. In this case, the pipe jacking method used fiber duct in concrete and can be defined by 5.2, 0.91 and 0.010, respectively.

$$T_4^{''}=\frac{\rho}{2\pi}\ln\frac{D_o}{D_d} \quad (11)$$

where ρ represents the thermal resistivity of duct material.

$$T_4^{'''}=\frac{\rho_c}{2\pi}\left(\ln\frac{D_x}{D_d}+\mu\ln\frac{4L\cdot F}{D_x}\right)+\mu\frac{N}{2\pi}(\rho_e-\rho_c)G_b \quad (12)$$

So, the cable current rating equation of the condition with moisture migration (Equation (4)) can be modified by adding the terms: $\left(\upsilon-1\right)\Delta\theta_x$ and υT_4 for T_4, respectively.

(13)

$$I=\left[\frac{\theta_C-\theta_{amb}-W_d\left[0.5T_1+n\left(T_2+T_3+\upsilon T_4\right)\right]+\left(\upsilon-1\right)\Delta\theta_x}{RT_1+nR\left(1+\lambda_1\right)T_2+nR\left(1+\lambda_1+\lambda_2\right)\left(T_3+\upsilon T_4\right)}\right]^{0.5}$$

Economic analysis

The cost of constructing underground power cables is divided into direct and indirect costs. However, determining the indirect cost can be challenging due to various uncontrollable parameters such as site facilities, interest expenses, duty stamps, land rental, and more. The direct cost, which encompasses materials, machinery, and labour, plays a pivotal role in the construction process. The capital cost can be mathematically represented as equation (14).

$$\text{Capital Cost} = DC + IDC \quad (14)$$

where DC is the direct cost and IDC is the indirect cost.

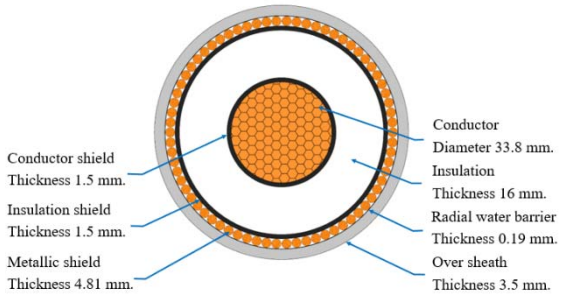

Fig.2. Structure of the underground power cables

Underground Power Cables

In this paper, the focus was on a 115 kV transmission line utilizing an 800 sq.mm. power cable specification, which was employed for the purpose of transitioning from an overhead line to an underground system. The ongoing

construction of MEA's Ratchadaphisek-Rama 9 project served as the context for this study. The structures and parameters related to the underground power cables are illustrated in Figure 2 and outlined in Table 1.

Table 1. Material thermal resistance

Structure	Material	Thermal Resistance $(K \cdot m / W)$
Conductor	Copper	2.5E-3
Conductor shield	XLPE	3.50
Insulation	XLPE	3.50
Insulation shield	XLPE	3.50
Metallic shield	Copper	2.50E-3
Water barrier	Aluminum	4.20E-3
Over sheath	PE	3.50
RTRC Conduit	Fiber glass	4.80
Air space	Air	40.00
Concrete pipe	Concrete	1.00
Mortar grouting	Concrete	1.00
Cable racks	Steel	13.00E-3
Soil	Soil	1.00
Water	Water [29]	0.001

Underground power cables installation

The underground power cables installation is a crucial point in reality, especially if the site location is in a big city that is linked by underground power cables on a regular basis. The traffic in roads and location are the main problems for selecting the installation method of the underground power cables. The transmission line system can be presented by the MEA's transmission line system that consists of 1) terminal station, 2) transmission line, and 3) substation. This research focused on the underground duct banks between the terminal station and the substation, as shown in Figure 3.

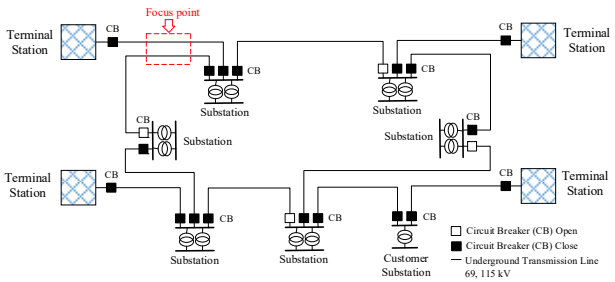

Fig.3. Single line diagram of the underground transmission line system

The focus point in Figure 3 is presented in Figure 4. The electric manhole and the concrete duct banks are the main structures of the underground duct banks. The electric manhole is essential both during and after construction. A manhole is used to install a pipe jacking machine during the construction period. After the construction of the manhole is completed, it is used as the cable connection point. Excavation of the road surface for the construction of manholes affects the traffic and people and may cause serious accidents.

This study focused on the cylindrical duct bank and square tunnel concrete to evaluate the ampacity and cost of underground power cables installation. The cylindrical duct bank was constructed by the pipe jacking method with Reinforced Thermosetting Resin Conduit (RTRC) as shown in Figure 4.

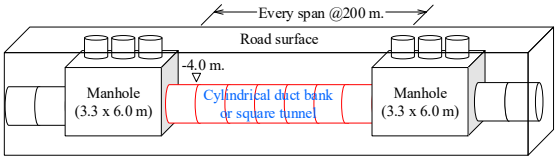

Fig.4. Construction of the underground power cables in Thailand by using the pipe jacking method

The cylindrical duct bank is constructed with cylindrical concrete pipes. The construction process consists of: 1) Installing concrete pipe by pipe jacking method, 2) Installing RTRC within the concrete pipes, and grouting mortar concrete to fill the gap around the RTRC, as shown in Figure 4. The concrete duct banks were constructed with this method, as shown in Figure 5.

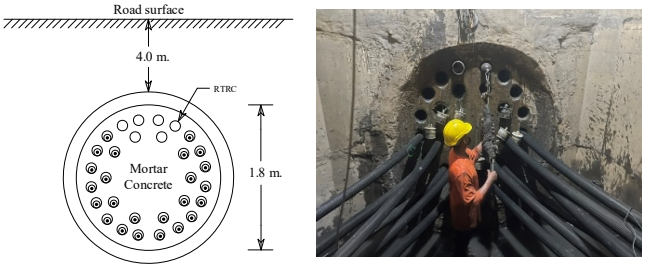

a) Trefoil formation cable arrangement

b) cylindrical duct bank installation fields

Fig.5. Cylindrical duct bank for the underground power cable installation

Meanwhile, the square tunnel is constructed with square concrete pipes. In contrast, the square tunnel uses cable racks for supporting underground power cables and does not add concrete mortar inside the pipe. The concrete pipes are installed 4 m. below the traffic surface, which has the same pattern as the cable trench of the substation, as shown in Figure 6.

Fig.6. Square tunnel for the underground power cable installation

The study of square tunnel in this research considered the arrangements of flat and trefoil power cables. Flat cable arrangement formation had 6 conductors per circuit, providing space for a power cable of 24 kV and communication cables, as shown in Figure 5. The square tunnel could support a maximum of 4 transmission lines. Trefoil cable arrangement formation had 6 conductors per circuit, providing space for a power cable of 24 kV and communication cables, the square tunnel could support a maximum of 6 transmission lines, as shown in Figure 7.

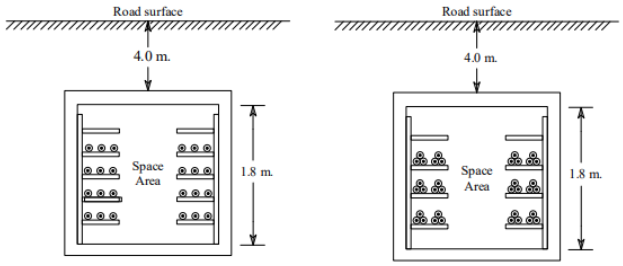

Fig.7. Cable arrangement of square tunnel for the underground power cable installation

Case Study

The case study of simulation was performed using the finite element method. At the same time, the costs of construction from the price collection and procedure of the construction project were calculated. Therefore, the case study can be defined as follows:

Case 1: Reliability verification of the finite element method (FEM) compared to MEA's standard ampacity.

Case 2: Simulating the heat effect on the ampacity of the power cables installed in the cylindrical duct bank and the square tunnel in non-flooding conditions with flat and trefoil arrangements of power cables.

Case 3: Simulating the heat effect on the ampacity of the power cables installed in the cylindrical duct bank and the square tunnel in flooding conditions with flat and trefoil arrangements of power cables.

Case 4: Comparing the simulation results of the power cables installed inside the cylindrical duct bank and the square tunnel of the cable arrangement for each formation in the case of non-flooding and flooding conditions.

Case 5: The comparison of cost calculation between the cylindrical duct bank and the square tunnel.

Simulation and Results

To confirm the adequacy of the simulation of each case study, its verification was made using numerical simulation in the software and data correction can be presented as follows.

Case 1:

The ampacity simulation comparison to the MEA's standard revealed that the simulation result was remarkably close to the standard value [30]. The simulation results are shown in Table 2.

Table 2 presents the ampacity values for 800 sq.mm. 115 kV power cables, categorized by the number of conductors. The ampacity values are provided for both MEA's standard and finite element method (FEM) calculations. The comparison highlighted the following percentage errors between the two methods: -0.24% for 6 conductors, 1.67% for 12 conductors, 1.06% for 18 conductors, and 0.99% for 24 conductors.

Table 2. Ampacity of the power cables 800 sq.mm. 115 kV

Number of conductors	Ampacity (A)		% Error
	MEA's standard	FEM	
6	831	829	-0.24
12	658	669	1.67
18	564	570	1.06
24	504	509	0.99

Case 2:

The simulation results of the underground power cables installed inside the cylindrical duct bank and the square tunnel were discussed in the non-flooding condition. The simulation results showed that the power cables installed in the cylindrical duct bank carried the highest load because the power cables were enclosed by concrete, which has low thermal resistance. On the other hand, the power cables installed inside the square tunnel arranged a trefoil cable formation bore the least electrical load because the heat accumulated between the cables and poor heat transfer due to the surrounding air of the power cables having a high thermal resistance. At the same time, the power cable installed inside the square tunnel arranged in a flat cable formation carried more electrical loads because no heat accumulated between the power cables. The simulation results are shown in Table 3.

Table 3. Ampacity comparison of the power cables, installation of cylindrical duct bank and square tunnel at non-flooding condition

Number of conductors	Ampacity (A)		
	Cylindrical duct bank	Square tunnel	
	Trefoil	Flat	Trefoil
6	829	748	725
12	669	652	637
18	570	532	520
24	509	494	483
30	-	-	426
36	-	-	405

Table 3 offers a comprehensive ampacity comparison for power cables in two distinct settings: a cylindrical duct bank and a square tunnel, both operating under non-flooding conditions. Ampacity values were detailed across varying conductor quantities and cable configurations. The cylindrical duct bank setup yielded ampacity figures ranging from 829 A to 509 A, correlating with an increased number of conductors. In contrast, a comparison between two cable configurations: trefoil and flat was presented in the square tunnel condition presents. Ampacity values for the square tunnel spanned from 725 to 405 A, demonstrating an ascending pattern with greater conductor counts. Notably, specific values for 30 and 36 conductors were absent in the square tunnel context.

The thermal simulation results for power cables installed in both the cylindrical duct bank and the square tunnel were examined under non-flooding conditions. The simulation findings revealed that power cables in the cylindrical duct bank exhibited lower heat generation. Conversely, power cables installed in the square tunnel with a trefoil cable arrangement resulted in higher heat generation. Simultaneously, power cables arranged in a flat configuration within the square tunnel experienced less heat generation compared to one with the trefoil configuration. The corresponding simulation results are illustrated in Figure 8.

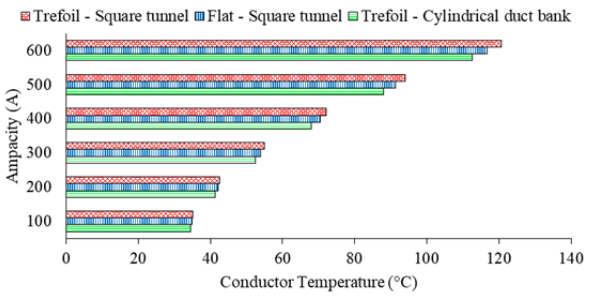

Fig.8. Conductor temperatures at various ampacity of different installations in non-flooding conditions

Case 3:

This section delves into the simulation outcomes of underground power cables installed in a cylindrical duct

bank and a square tunnel in flooding conditions. The results revealed that power cables in the square tunnel, arranged in a flat cable configuration, bore the highest load due to water immersion, resulting in low thermal resistance. Conversely, the trefoil cable arrangement in the square tunnel exhibited a lower ampacity than one with the flat configuration. In contrast, power cables in the cylindrical duct bank carried a minimal electrical load due to the higher thermal resistance of concrete compared to water. The corresponding simulation results are detailed in Table 4.

Table 4. The ampacity comparison of the power cables installed in the cylindrical duct bank and the square tunnel in flooding conditions

Number of conductor	Ampacity (A)		
	Cylindrical duct bank	Square tunnel	
	Trefoil	Flat	Trefoil
6	912	1,112	1,108
12	697	811	810
18	590	668	600
24	523	579	577
30	-	-	478
36	-	-	445

The thermal simulation results of the power cables installed in the cylindrical duct bank and the square tunnel were discussed in the flooding conditions. The simulation results showed that the power cables installed in the square tunnel and arranged in the flat cable formation had the least heat. On the other hand, the power cables installed in the cylindrical duct bank had higher heat. At the same time, the power cables installed in the square tunnel and arranged in the trefoil cable formation had higher heat than one with the flat cable formation. The simulation results are shown in Fig. 9.

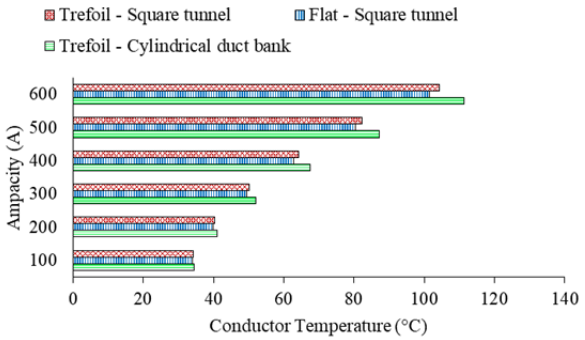

Fig.9. Conductor temperatures at various ampacity of different installations in flooding conditions

Case 4:

Figure 10 illustrates the computational domain utilized for the cylindrical duct bank simulation, while Figure 11 displays the finite element mesh within this domain. An automated mesh approach was adopted due to minimal mesh size impact on temperature results. The arrangement of power cables within the cylindrical duct bank shown in Figure 12 had a three-phase power system, with two conductors per circuit and four circuits. The blank conduits accommodated 24 kV power and communication cables. Simulation outcomes revealed heat concentration on the inner conductor due to neighboring conductor blockage, resulting in poor heat dissipation. Furthermore, heat dispersed more profoundly into the deep soil layer than the surface, which is attributed to the lower temperature of the former. Notably, a conductor temperature of 90°C, in line with cable ratings, supported 509 A under non-flooding and 523 A during flooding conditions.

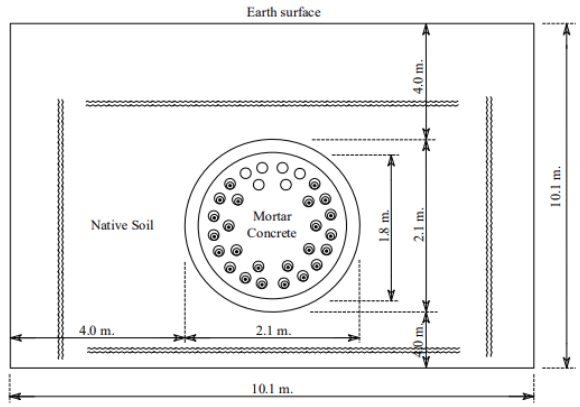

Fig.10. Dimension of the computational domain for the cylindrical duct bank

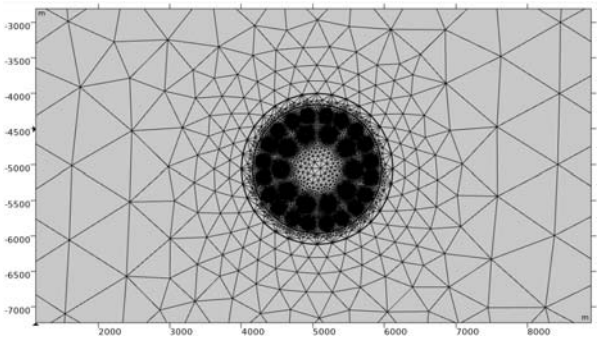

Fig.11. Finite element mesh generated within the portion of the domain in Fig.10

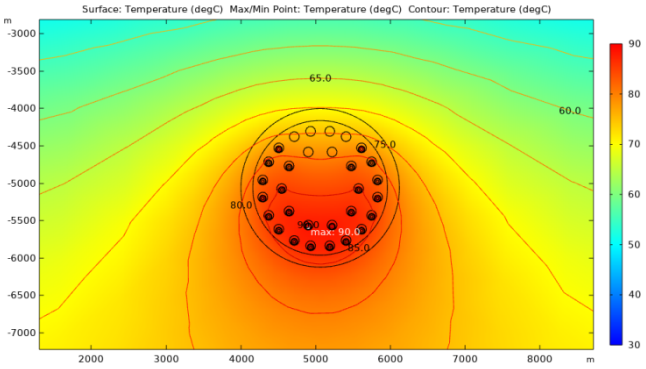

Fig.12. Simulation results of temperature for the cylindrical duct bank installation

Figure 13 depicts the computational domain utilized for the square tunnel simulation, while Figure 14 showcases the finite element mesh generated within a specific portion of this domain. An automated meshing approach was adopted due to the minimal impact of mesh size on temperature outcomes. The arrangement of power cables within the square tunnel is illustrated in Figure 15, which had a three-phase power system with two conductors per phase and a total of six circuits. The empty cable racks supported both 24 kV power cables and communication cables. Simulation results revealed that heat generation within the conductor significantly accumulated in the cables arranged in a trefoil formation. This setup presented challenges in dissipating the accumulated heat outward. Additionally, heat dispersion into the deep soil layer was more pronounced compared to the surface due to the lower temperature of the deeper soil. Considering cable ratings, a conductor temperature of 90°C supporting an ampacity of 405 A during non-flooding conditions increased to 445 A in flooding conditions.

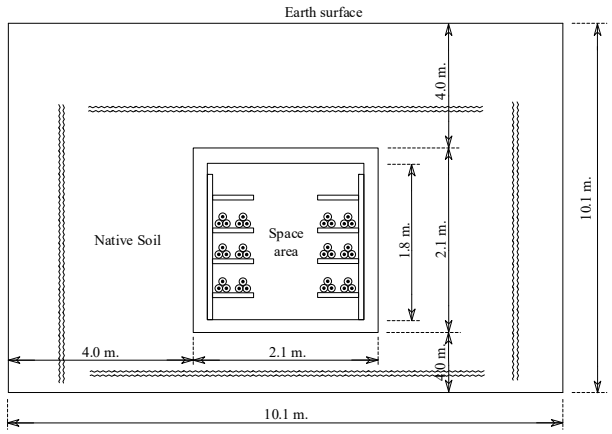

Fig.13. Dimension of the computational domain for the square tunnel

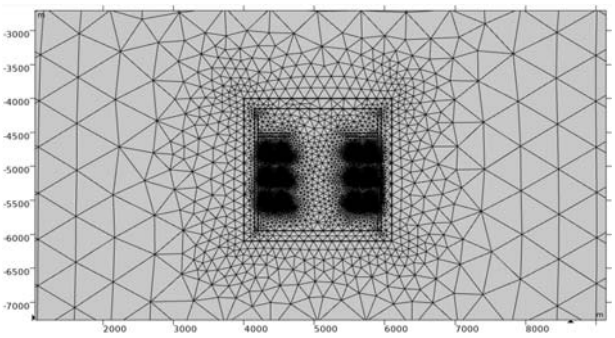

Fig.14. Finite element mesh generated within the portion of the domain in Fig.13

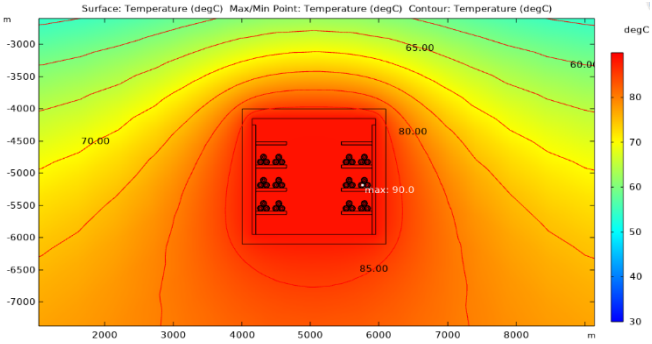

Fig.15. Simulation results of temperature for the square tunnel installation

Case 5:

This paper calculated the capital cost at a distance of 1,000 m for comparison. The construction of the cylindrical duct bank and the square tunnel require different materials and processes. The study results showed that the cylindrical duct bank used RTRC to support the power cables and was covered by concrete mortar. On the contrary, the square tunnel used the cable racks and the cable cleats instead. The load-bearing behavior of the cylindrical concrete pipe was stronger than that of the square concrete pipe. Therefore, the square concrete pipe needed to be reinforced with steel to yield the same strength, making it more expensive than the cylindrical concrete pipe.

Table 5 presents a breakdown of costs for two methods of implementing an underground power cable system: a cylindrical duct bank and a square tunnel. The costs were expressed in US dollars ($). The cost calculation assumed an exchange rate of 33.46 Thai baht to $1. It was observed that the cylindrical duct bank option was more cost-effective compared to the square tunnel. The cylindrical duct bank had the capacity to support transmission lines of 115 kV for up to 4 circuits. In contrast, the square tunnel could accommodate up to 6 circuits. Consequently, when comparing the cost per circuit, the analysis revealed that the square tunnel was less expensive than the cylindrical duct bank. In summary, the cost analysis suggests that the cylindrical duct bank had lower overall costs, albeit with a higher cost per circuit compared to the square tunnel. It is worth emphasizing that the selection between these options should take into consideration not only financial aspects but also factors such as system performance, construction timelines, and other relevant considerations.

Table 5. Capital cost of the duct bank per 1 km.

Description	Cost ($)	
	Cylindrical duct bank	Square tunnel
Design	5,230	5,230
Topographic survey	2,989	2,989
Traffic management	10,460	10,460
Manhole work	560,789	560,789
Pipe jacking work	1,053,796	1,214,585
Inner duct (RTRC)	350,269	-
Grouting work	286,611	-
Cable racks	-	118,350
Cable cleats	-	490,137
Pavement	23,640	23,640
Summary cost	2,293,784	2,426,180
Cost per circuit	573,446	404,363

Conclusion

This paper successfully conducted a comparative analysis of the capital costs and ampacity of underground power cables between cylindrical duct banks and square tunnels installations, as presented below:

1.Simulation results obtained through the finite element method demonstrated that the ampacity closely aligned with the standards set by the Metropolitan Electricity Authority (MEA) in Thailand.

2.Under non-flooding conditions, the ampacity of underground power cables was affected by their arrangement. In a cylindrical duct bank, a trefoil formation arrangement offered the highest current-carrying capacity. Conversely, a flat formation arrangement in a square tunnel yielded a lower current, while the trefoil arrangement in a square tunnel resulted in the lowest current.

3.When flooding occurred, the arrangement's impact on ampacity remained significant. In a square tunnel, a flat formation arrangement allowed for the highest current capacity. On the other hand, a trefoil formation arrangement in a square tunnel led to a lower current capacity, whereas the trefoil arrangement within a cylindrical duct bank yielded the least current capacity.

4.Following the standards of the Metropolitan Electricity Authority (MEA), electrical conduits are necessary for medium voltage cables. For 800 sq. mm transmission power cables, with six cables per circuit, a cylindrical duct bank could accommodate 4 circuits, while a square tunnel could manage 4 circuits with a flat arrangement or 6 circuits with a trefoil arrangement.

5.Using a square tunnel with the pipe jacking method resulted in a 5.77% higher capital cost compared to constructing a cylindrical duct bank. However, the average construction cost per circuit was 29.49% lower.

Because Bangkok ground level is situated 1.50 m above mean sea level (MSL), the duct banks are positioned at a minimum depth of 4 m beneath the traffic surface, therefore, an extended rainy season results in frequent flooding of underground power cables. The use of a square tunnel for the power cable system, thus, emerges as a feasible alternative. However, it is important to consider a range of other factors, including construction timelines, in the decision-making process.

***Authors**: Assoc. Prof. Dr. Boonyang Plangklang, Department of Electrical Engineering, Rajamangala University of Technology Thanyaburi (RMUTT) 12110 Thailand. Corresponding author's Email: boonyang.p@en.rmutt.ac.th;*
Mr. Ritthichai Ratchapan, Department of Electrical Engineering, Rajamangala University of Technology Thanyaburi (RMUTT) 12110 Thailand. Email: ritthichai_r@mail.rmutt.ac.th;
Mr. Somchai Kriprab, Department of Electrical Engineering, Rajamangala University of Technology Thanyaburi (RMUTT) 12110 Thailand. E-mail: somchai_k@mail.rmutt.ac.th;
Dr. Supapradit Marsong, Department of Electrical Engineering, Rajamangala University of Technology Thanyaburi (RMUTT) 12110 Thailand. E-mail: supapradit_m@mail.rmutt.ac.th;
Asst.Prof.Dr. Yuttana Kongjeen, Department of Electrical Engineering, Rajamangala University of Technology Isan (RMUTI) 3000 Thailand. E-mail: yuttana.ko@rmuti.ac.th

REFERENCES

[1] Bascom, Williams, and Kwilinski, "Technical considerations for applying trenchless technology methods to underground power cables," in *2016 IEEE/PES Transmission and Distribution Conference and Exposition (T&D)*, 2016: IEEE, pp. 1-5.
[2] Rajakrom, "Undergrounding the Power Distribution Network in Luang Prabang World Heritage," *GMSARN International Journal* vol. 5, pp. 37-44, 2011.
[3] Att Phayomhom, "Analysis of Electric Field and Magnetic Field from Overhead Subtransmission Lines Affecting Occupational Health and Safety in MEA's Power System," *GMSARN International Journal,* vol. 10, pp. 25-32, 2016.
[4] Jian, Huan, Xiao, and Xu, "Ampacity analysis of buried cables based on electromagnetic-thermal finite element method," in *2018 2nd International Conference on Smart Grid and Smart Cities (ICSGSC)*, 2018: IEEE, pp. 73-79.
[5] Bossio, Lengwiler, Heimbach, Kälin, Fauci, and Casura, "Sensitivity analysis of cable trench modelling with concrete duct bank and multiple material layers for the current rating of 150kv cables," in *CIRED 2021-The 26th International Conference and Exhibition on Electricity Distribution*, 2021, vol. 2021: IET, pp. 332-336.
[6] Pradipta and Hudaya, "Effects of depth burial on current carrying capacity of XLPE 86/150 (170) kV underground cable," in *2018 International Conference on Information and Communications Technology (ICOIACT)*, 2018: IEEE, pp. 506-510.
[7] Earle, Rusty, and Rezutko, "Novel installation of a 138kV pipe-type cable system under water using horizontal directional drilling," in *T&D Conference and Exposition, 2014 IEEE PES.*, 2014.
[8] Zhu *et al.*, "Thermal Effect of Different Laying Modes on Cross-Linked Polyethylene (XLPE) Insulation and a New Estimation on Cable Ampacity," *Energies,* vol. 12, no. 15, 2019, doi: 10.3390/en12152994.
[9] Colef and de Leon, "Improvement of the Standard Ampacity Calculations for Power Cables Installed in Trefoil Formations in Ventilated Tunnels," *IEEE Transactions on Power Delivery,* vol. 37, no. 1, pp. 627-637, 2022, doi: 10.1109/tpwrd.2021.3068111.
[10] Shang, Xu, and Xue, "Application of guided boring trenchless technology on pipeline cross railway," in *2011 International Conference on Multimedia Technology*, 2011: IEEE, pp. 975-978.
[11] Hoerauf, "Ampacity Application Considerations for Underground Cables," *IEEE Transactions on Industry Applications,* vol. 52, no. 6, pp. 4638-4645, 2016, doi: 10.1109/tia.2016.2600656.
[12] Charerndee, Chatthaworn, Khunkitti, Kruesubthaworn, Siritaratiwat, and Surawanitkun, "Effect of concrete duct bank dimension with thermal properties of concrete on sensitivity of underground power cable ampacity," in *2018 18th International Symposium on Communications and Information Technologies (ISCIT)*, 2018: IEEE, pp. 484-489.
[13] Fu, Si, Quan, and Yang, "Numerical Study of Heat Transfer in Trefoil Buried Cable with Fluidized Thermal Backfill and Laying Parameter Optimization," *Mathematical Problems in Engineering,* vol. 2019, pp. 1-13, 2019, doi: 10.1155/2019/4741871.
[14] Klimenta, Perović, Klimenta, Jevtić, Milovanović, and Krstić, "Modelling the thermal effect of solar radiation on the ampacity of a low voltage underground cable," *International Journal of Thermal Sciences,* vol. 134, pp. 507-516, 2018, doi: 10.1016/j.ijthermalsci.2018.08.012.
[15] Perka, "Przegląd metod modelowania przepływu ciepła w przewodach elektrycznych," *PrzeglĄd Elektrotechniczny,* vol. 1, no. 7, pp. 92-95, 2021, doi: 10.15199/48.2021.07.18.
[16] MaŚNicki, "Odprowadzanie ciepła z kabla w podziemnych liniach elektroenergetycznych," *PrzeglĄd Elektrotechniczny,* vol. 1, no. 5, pp. 76-79, 2021, doi: 10.15199/48.2021.05.12.
[17] Anders and Brakelmann, "Rating of Underground Power Cables With Boundary Temperature Restrictions," *IEEE Transactions on Power Delivery,* vol. 33, no. 4, pp. 1895-1902, 2018, doi: 10.1109/TPWRD.2017.2771367.
[18] Gouda, Dein, and Amer, "Effect of the Formation of the Dry Zone Around Underground Power Cables on Their Ratings," *IEEE Transactions on Power Delivery,* vol. 26, no. 2, pp. 972-978, 2011, doi: 10.1109/TPWRD.2010.2060369.
[19] Diaz-Aguiló, León, Jazebi, and Terracciano, "Ladder-Type Soil Model for Dynamic Thermal Rating of Underground Power Cables," *IEEE Power and Energy Technology Systems Journal,* vol. 1, pp. 21-30, 2014, doi: 10.1109/JPETS.2014.2365017.
[20] Brakelmann and Anders, "Ampacity Calculations of Underground Power Cables With End Effects," *IEEE Transactions on Power Delivery,* vol. 38, no. 3, pp. 1968-1976, 2023, doi: 10.1109/tpwrd.2022.3229585.
[21] Kropotin, "Mathematical model of XLPE insulated cable power line with underground installation," *PrzeglĄd Elektrotechniczny,* vol. 1, no. 6, pp. 79-82, 2019, doi: 10.15199/48.2019.06.14.
[22] Czapp, "Effect of soil moisture on current-carrying capacity of low-voltage power cables," *PrzeglĄd Elektrotechniczny,* vol. 1, no. 6, pp. 156-161, 2019, doi: 10.15199/48.2019.06.29.
[23] Anders, "Wpáyw skrzyĪowania linii kablowych wysokiego napiĆcia 110 kV na ich dáugotrwaáą obciąĪalnoĞü prądową," *PrzeglĄd Elektrotechniczny,* vol. 1, no. 5, pp. 121-125, 2019, doi: 10.15199/48.2019.05.29.
[24] Bustamante *et al.*, "Thermal behaviour of medium-voltage underground cables under high-load operating conditions," *Applied Thermal Engineering,* vol. 156, pp. 444-452, 2019, doi: 10.1016/j.applthermaleng.2019.04.083.
[25] Cheng, "Emergency Capacity Prediction of Direct Buried Cable under Rainfall Condition," in *2019 IEEE Innovative Smart Grid Technologies-Asia (ISGT Asia)*, 2019: IEEE, pp. 176-180.
[26] Charerndee, Chatthaworn, Khunkitti, Kruesubthaworn, Siritaratiwat, and Surawanitkun, "Investment Cost Analysis with Structural Design of Concrete Duct Bank Power Cables," in *IOP Conference Series: Materials Science and Engineering*, 2020, vol. 897, no. 1: IOP Publishing, p. 012007.
[27] Klimenta, Tasić, and Jevtić, "The use of hydronic asphalt pavements as an alternative method of eliminating hot spots of underground power cables," *Applied Thermal Engineering,* vol. 168, 2020, doi: 10.1016/j.applthermaleng.2019.114818.
[28] Klimenta, Jevtić, Andriukaitis, and Mijailović, "Increasing the transmission performance of a conventional 110 kV cable line by combining a hydronic concrete pavement system with photovoltaic floor tiles," *Electrical Engineering,* vol. 103, no. 3, pp. 1401-1415, 2021, doi: 10.1007/s00202-020-01167-4.
[29] COMSOL. "Inductive Heating of a Copper Cylinder." (accessed 15.08.2023, 2023).
[30] Metropolitan Electricity Authority (MEA) of Thailand. . (2020). *Power Cable Ampacities in Conduit with Pipe Jacking (Shielded Extruded Insulation CU Conductor, Rated 69 _ 115 kV) (UG-.pdf>*.